A hybrid particle filter-Weibull approach for probabilistic end-of-life prediction of industrial machines using vibration data

Nagesh Dewangan[1] and Amiya Ranjan Mohanty[2]

[1,2]*Department of Mechanical Engineering, Indian Institute of Technology Kharagpur, Kharagpur 721302, West Bengal, India*

nagesh@iitkgp.ac.in
amohanty@mech.iitkgp.ac.in

ABSTRACT

Accurate degradation modeling is essential for ensuring the reliability of industrial machinery operating under uncertain conditions. This paper presents a hybrid prognostic framework that integrates Particle Filters (PF) with a Weibull Failure Rate Function (WFRF) for probabilistic End-of-Life (EOL) prediction using vibration data. The PF is employed to estimate hidden degradation states and update model parameters sequentially, while the WFRF provides a statistical representation of failure behavior. The proposed framework enables joint degradation tracking and uncertainty quantification. The method is validated using vibration datasets from a mining dumper operating under real conditions and from an induction motor operating under controlled laboratory conditions. Results demonstrate that the hybrid PF-WFRF approach achieves accurate EOL prediction with small deviation from actual failure thresholds (within ~120 seconds) and provides meaningful uncertainty bounds through probability density functions. Unlike existing hybrid approaches that rely on machine learning, the proposed framework provides a computationally efficient, interpretable probabilistic solution. The framework is robust to both smooth and noisy degradation signals, making it suitable for real-world prognostics applications.

1. INTRODUCTION

Reliability and availability of components are crucial for the smooth operation of industrial machines. The machines operate under various unpredictable conditions, including fluctuating loads, speed variations, and environmental factors, which can lead to component deterioration over time. The degradation of their components causes not only inefficiency in task completion but also deterioration of other connected components. Therefore, continuous monitoring is necessary to assess degradation levels and estimate End-of-Life (EOL), ensuring smooth operation. This is possible through sensors that monitor their deteriorating health over time. Some of the machine's key components include engines and electric motors that operate continuously to perform various tasks. The mechanical components of these machines are often affected by working conditions, such as high loads, vibrations, temperature fluctuations, and environmental factors, which accelerate degradation processes and ultimately lead to unexpected failures if not detected in a timely manner. Any unplanned downtime caused by mechanical failures, due to degradation, can result in substantial production losses and increased operational costs. Prolonged use of degraded lubricating oil or clogged filters can be highly detrimental to machines, as it accelerates wear and tear of critical components and significantly reduces their operational lifespan. On the other hand, a deteriorating component can further degrade other connected components. Therefore, it is essential to estimate and predict component degradation using historical data, such as vibration measurements, to enable maintenance scheduling based on the estimated time to failure and to estimate the next downtime.

Dumpers are operated to transport material within surface coal mines under very harsh conditions, which, over time, cause component deterioration and degradation of lubricating oil (Dey et al., 2017; Santana, 2022). The degradation and health of machines are monitored through various methods, notably oil and vibration analysis. Oil analysis detects internal wear and lubricant condition (Siddiqui et al., 2021), whereas vibration analysis captures mechanical faults such as misalignment and bearing wear, making them highly effective for Condition-Based Maintenance (CBM) (Rai & Mohanty, 2007). Dewangan et al. (2019) examined the properties of lubricating oil, such as viscosity, that change due to its degradation. Furthermore, Santana et al. (2019) investigated the relationship between lubricant properties and vibration analysis, noting an increase in vibration level due to lubricant deterioration. Later, they explored vibration analysis on different

https://doi.org/10.36001/IJPHM.2026.v17i2.4735

lubricating oils (Santana, 2022). They have also mentioned an intense increase in vibration levels beyond the manufacturer's recommended usage within the viscosity limit. However, they have not measured the degradation in the frequency band. Furthermore, Gupta et al. (2020) conducted vibration analysis of gear systems using lubricating oils to assess vibration levels under various lubrication conditions, including frequency analysis. They have shown the Root Mean Square (RMS) vibration level in the frequency spectrum to identify the effect of lubrication conditions on vibration. These studies confirmed that lubricating oil degradation should be investigated using vibration analysis.

Similarly, electric motors are essential for the smooth and uninterrupted operation of mechanical equipment across various industries, including those involving conveyors and compressors. They are affected by wear, fatigue, imbalance, and misalignment due to prolonged usage (Pradhan, 2014). Motors have several components, with bearings being the most critical. Researchers have demonstrated that bearing faults and their degradation can be effectively monitored using vibration analysis. PRONOSTIA dataset is one of them, which has multiple run-to-failure vibration datasets (Nectoux et al., 2012). Moreover, other researchers also explored bearing degradation using various models (Qiu et al., 2006; Zhu et al., 2022). Bearing failure is often caused by multiple faults, including those in the ball, cage, inner race, and outer race, which can degrade over time. Furthermore, the motor's other components, such as the stator, rotor bar, eccentricity, and torque fluctuation, can significantly impact overall system performance, as examined by Pal et al. (2023). Moreover, Mohanty et al. (2012) conducted vibration analysis to detect a broken impeller fault at various levels in a pump. They highlighted the detection of impeller damage levels at various stages using vibration analysis. Therefore, these faults should be studied over a long period to determine the degradation trend and failure caused by each fault, because any fault in the motor affects the bearing components.

Furthermore, researchers have employed various methods to determine the degradation trend in data and estimate the posterior trend or Remaining Useful Life (RUL) from prior data. These methods range from model-based to data-driven and hybrid models. Model-based approaches describe the underlying physical phenomena and failure mechanisms that drive degradation and have been applied to diverse components, such as valves, bearings, and metallic structures. While they provide high interpretability, are physically meaningful, and exhibit good generalization if accurately modeled, physics models are often computationally demanding, constrained by simplifying assumptions, and difficult to validate, which limits their application to complex systems.

Data-driven models learn degradation patterns from historical sensor data, eliminating the need for expert knowledge of the system. Their flexibility and general applicability across components have made them the dominant approach in the prognostics field. While they offer scalability for large datasets and avoid the need for models, they suffer from unrepresentative data, limited interpretability, and limited generalizability to unseen conditions. Data-driven models primarily fall into three categories: Machine Learning (ML), stochastic models, and Sequential models, each with its own advantages and disadvantages (Hachem et al., 2024). ML methods, such as Support Vector Machines (SVRs), Long Short-Term Memory (LSTMs), Convolutional Neural Networks (CNNs), Neural Networks (NNs), and Random Forests (RFs), are widely used for posterior predictions; however, they require large amounts of data. So, they are not applicable to applications with smaller data. Moreover, epistemic uncertainty and point estimates with MLs limit their predictive capabilities. Additionally, predictions from ML models are often black-box and less interpretable, requiring explainability tools such as Shapley Additive Explanations (SHAP) and Local Interpretable Model-agnostic Explanations (LIME) for interpretation. In comparison, XGBoost has been adopted in prognostics due to its ability to learn nonlinear degradation patterns from relatively small datasets while maintaining high computational efficiency (Chen & Guestrin, 2016). A recent study has demonstrated its effectiveness in RUL estimation for lithium-ion batteries, making it an appropriate ML baseline for comparison with the proposed Particle Filter (PF) - Weibull Failure Rate Function (WFRF) framework (Jin et al., 2025). Later, stochastic methods, such as Weibull, Gamma, Lognormal, Wiener, and Hidden Markov Models, are more suitable for smaller datasets, offering better interpretability and fewer computations. These models are inherently probabilistic and robust when the correct model is selected. However, they do not provide a distribution of posterior predictions, which limits the independent use of the stochastic models. Moreover, they are unable to accommodate complex data trends. Therefore, these limitations of applicability, stemming from limited data and posterior prediction distributions, are addressed by Sequential models. Sequential models, such as PF, Unscented Kalman Filter (UKF), and Bayesian Filter (BF), do not require a large amount of data and help define the probability distribution of predictions when combined with stochastic models. Further, they update predictions based on the arrival of new data, handle noisy measurements, and provide a probabilistic state estimate. They are often used for real-time tracking and prognosis. However, some BF models are computationally expensive and require accurate state-space models and assumptions about model noise. Overall, data-driven methods are widely used in prognostics and health monitoring applications, including machinery RUL prediction, fault detection, reliability analysis, structural health monitoring, battery health assessment, maintenance planning, industrial Internet of Things (IoT) monitoring, electronic component, automotive, and robotics prognostics, aircraft engine maintenance, biomedical survival analysis, and navigation and tracking systems.

Recently, hybrid prognostic approaches have attracted considerable attention because they combine the advantages of physics-based and data-driven methods while reducing their individual limitations (Rezamand et al., 2020). Hybrid frameworks integrate degradation models, physical knowledge, stochastic methods, and machine learning algorithms to improve prediction accuracy and uncertainty quantification, and solve the problem of interpretability and generalization while working on a smaller data size (Cuesta et al., 2025). Several studies have combined PF and KF with stochastic methods or Physics-Informed Neural Network (PINN) to estimate degradation states and reduce prediction uncertainty (Wang, He, et al., 2021; Wang, Peng, et al., 2021). Furthermore, Weibull-based degradation models have been extensively employed in reliability engineering and prognostics because of their ability to represent increasing, decreasing, and constant degradation rates (Rathore & Harsha, 2022). Weibull model provides physically interpretable parameters associated with the degradation process and failure characteristics. Even XGBoost has been combined with PF-KF to estimate RUL of lithium-ion batteries (Jafari & Byun, 2022). Therefore, it has been implemented to prognose bearings, gears, and cutting tools, estimate the RUL of these elements under operating conditions, and suggest effective replacement decisions (Cameron & Krantz, 2023; Souza et al., 2025; Kundu et al., 2019). Therefore, a hybrid framework that combines a probabilistic stochastic model with a Bayesian filter can effectively address the shortcomings of each method when applied independently. The comparison of methodological characteristics of data-driven models is presented in Table 1, and the evaluation methods for these models are provided in Table 2 (Guo et al., 2020; Khan et al., 2024; Khine et al., 2025; Salinas-Camus et al., 2025).

Previously, researchers have implemented hybrid frameworks for EOL estimation. Cheng et al. explored a hybrid prognostics approach to estimate the RUL of a planetary gearbox with a crack in a sun gear tooth (Cheng, 2015). They simulated vibration responses of both healthy and cracked gears and used a two-step statistical feature selection and weighting algorithm to identify the most sensitive and stable condition indicators. They have modified the Grey model by incorporating a residual term derived from simulation data. However, they did not present the prediction curve, leaving the posterior distribution of the estimates unclear. Further, experimental data have not been utilized because the simulation and experimental signals differ significantly. Therefore, this paper examines posterior estimates of the degradation of used machine components using experimental data. Ahmad et al. (2017) presented a hybrid model that combines a particle filter-based state-space model with a Support Vector Regression (SVR) predictor to monitor degradation under uncertain conditions. They demonstrated improved accuracy compared to individual methods in handling noise, nonlinearity, and degradation rates. However, the examined combination was computationally intensive and required substantial data to implement the ML model. Li et al. (2021) investigated a hybrid prognostics approach combining an Interacting Multiple Model Particle Filter (IMM-PF) with SVR for multi-step RUL estimation of Lithium-ion batteries. They used polynomial and exponential degradation models within the IMM framework and SVR to predict future measurements, addressing the lack of long-term data. However, computational burden is very high due to the implementation of ML models, particle filter, and SVR methods. Additionally, a more generalized model should be employed to analyze degradation trends. Kang et al. (2021) developed a Multilayer Perceptron (MLP) neural network framework to predict equipment RUL. They investigated a two-stage process that labeled data as healthy or failed based on the start and end of the dataset. However, they implemented linear regression for critical interpolation, which can be problematic for finding a degradation trend. Furthermore, their study used monotonic, noiseless run-to-failure data, which should be tested against non-monotonic, noisy degradation patterns. Skordilis et al. (2020) developed a real-time condition monitoring and prognostics system for deteriorating systems using a Hybrid State-Space Model (HSSM) with Extreme Machine Learning (EML). However, their method depended on the initialization step for the EML and PF parameters. Moreover, the method used had high computational requirements, which limited its practical application. To address these limitations, this paper proposes a hybrid approach combining a PF for degradation tracking with a Weibull model for efficient lifetime estimation and reliability analysis. This framework ensures both accuracy and computational efficiency, enabling continuous monitoring of equipment health and informed maintenance decisions, which are crucial for ensuring operational safety, minimizing unplanned downtime, and extending the overall lifespan of mining machinery. Moreover, previous studies have relied solely on NASA datasets for turbo engine (Li et al., 2018), battery (Fricke et al., 2023), and PRONOSTIA (Nectoux et al., 2012). Therefore, it is essential to investigate machine degradation using vibration signals from operational datasets of actual machines, such as dumpers and induction motors. Machines operating under various conditions generate distinct vibration signals that provide diagnostic information about their health. However, interpreting these signals under operational variability requires methods for assessing their health. Therefore, there is a need for robust probabilistic models that can capture uncertainty, nonlinearity, and hidden degradation states inherent in real industrial environments.

Despite these advancements, several important research gaps remain. First, there is a lack of robust probabilistic frameworks that integrate vibration-based degradation features with interpretable statistical models for EOL prediction in dumpers operating under harsh, noisy conditions. Second, existing vibration-based prognostic approaches for electric motors often assume simplified degradation models and fail to capture the stochastic, non-monotonic nature of real-world signals. Third, many hybrid models combine Bayesian filtering with machine learning techniques, increasing computational complexity and dependence on large datasets, thereby limiting their practical applicability. Fourth, statistical models, such as the Weibull distribution, are widely used for failure analysis due to their interpretability, but they are typically applied independently and do not account for dynamic degradation or uncertainty in state estimation. Finally, there is a lack of a framework capable of handling both smooth degradation behavior, as observed in motor experiments, and highly noisy vibration signals encountered in dumper operations using a hybrid approach.

Further, when the proposed framework is compared with individual modeling approaches in terms of their strengths, limitations, and Prognostics and Health Management (PHM). WFRF provides an interpretable statistical representation of degradation behavior; however, it is limited to deterministic trend modeling and does not capture uncertainty in state estimation. On the other hand, PF offers a probabilistic framework for handling noisy and nonlinear data, but it lacks an explicit failure model to describe the progression of degradation. The comparison of the proposed framework with the individual model is provided in Table 3.

Table 1. Methodological characteristics comparison of data-driven models

	Category		
	Machine Learning	Stochastic Models	Sequential Models
Methods	SVR, LSTM, etc.	Weibull, Gamma, etc.	PF, UKF, etc.
Principle	Learn patterns from historical or sensor data	Probabilistic degradation and RUL modeling	Sequential health state and RUL estimation
Advantages	Handles nonlinear relationship; Multimodal data learning; Scalable and automatic extract features	Probabilistic uncertainty and degradation modeling; Simple, interpretable, and data-efficient	Handle noisy measurements; Provide probabilistic state estimates in real-time; Handles partial observations
Disadvantages	Large datasets; Limited interpretability; Overfitting and poor generalization; High computational cost; Data dependent	Assumption dependent Limited for complex degradation Require degradation model Limited system flexibility	State-space model sensitive Computationally intensive Noise assumption sensitive Diverge with inaccurate model tuning

Table 2. Evaluation methods for data-driven models

	Category		
	Machine Learning	Stochastic Models	Sequential Models
Uncertainty	Weak: point estimates Extensions (Bayesian ML, ensembles, dropout) Epistemic uncertainty	Strong: inherently probabilistic Provides hazard rates	Very strong: Posterior state and RUL distributions Real-time aleatory + epistemic uncertainty
Robustness	Sensitive to noise, bias, and domain shift; Improved via regularization, ensembles, or domain adaptation	Robust under correct distributional assumptions; Sensitive to degradation deviations	High: Handles noisy and uncertain data; Sensitive to poor model assumptions or noise tuning
Interpretability	ML is treated as black box; Explainable via tools (SHAP, LIME, saliency maps)	Very high: Statistically interpretable parameters	Moderate: state variables are interpretable
Feasibility	Moderate to High: Data and compute dependent; Widely adopted in industrial IoT	High: simple to implement; Low computational and data requirement	Moderate: Real-time for low/medium-dimensions; Computational cost increases with complexity

Table 3. Comparison of prognostic approaches

Method	Strength	Limitation	PHM Capability
WFRF	Interpretable statistical model; captures degradation trend	Does not provide probabilistic state estimation	Limited (deterministic EOL only)
PF	Probabilistic state estimation; handles noise and nonlinearity	Lacks statistical failure model for degradation representation	Moderate (uncertainty without structured failure model)
PF-WFRF (Proposed)	Combines probabilistic estimation with statistical failure modeling	Slightly higher computational complexity	High (probabilistic EOL with uncertainty quantification)

To address these limitations, this study proposes a hybrid prognostic framework that integrates a PF with a WFRF for vibration-based EOL prediction. PF is employed to estimate hidden degradation states and update model parameters sequentially, enabling real-time tracking of degradation under uncertainty. The WFRF provides a statistically interpretable representation of failure characteristics, allowing reliable lifetime estimation and maintenance planning. The integration of these approaches enables simultaneous degradation modeling and probabilistic EOL prediction while maintaining computational efficiency and interpretability.

The main contributions of this work are as follows: (1) Development of a hybrid PF-WFRF framework for simultaneous degradation tracking and probabilistic EOL estimation; (2) Integration of statistical failure modeling with Bayesian sequential estimation to capture both aleatory and epistemic uncertainty; (3) Validation on both controlled (induction motor) and real-world (mining dumper) datasets demonstrating robustness under varying noise conditions; (4) Demonstration of probabilistic EOL prediction using vibration-based degradation features.

The paper is organized as follows: Section 2 describes WFRF and PF. Details of the proposed methodology are provided in Section 3. Section 4 presents the results of EOL estimation for the motor and the dumper. Section 5 discusses the findings and interprets the results. Section 6 provides conclusions and future research directions.

2. BACKGROUND

This section provides an overview of statistical and sequential models.

2.1. Weibull failure rate function (WFRF)

WFRF is a statistical distribution used in reliability engineering and failure analysis. It models the probability of failure over time and is defined by three parameters: shape (β) parameter defines the slope of degradation (decreasing, constant, or increasing); scale (α) parameter defines the characteristic life of degradation; and location (γ) parameter defines the time shift of the degradation, representing the earliest time at which failure can occur. For machine components, WFRF helps model nonlinear degradation, estimate failure time and EOL, and plan maintenance, due to its mathematical flexibility. Among stochastic degradation models, the WFRF is selected because its parameters (β, α) can represent varying degradation rates. This flexibility makes WFRF suitable for vibration degradation trends that evolve over different operating conditions. Furthermore, WFRF parameters have clear physical interpretations related to the degradation rate and characteristic life, which facilitate maintenance decision-making. It is particularly valuable for analyzing historical failure data to predict when a machine or component is likely to fail. The Eq. (1) represents WFRF.

$$Y = \frac{\beta}{\alpha}\left(\frac{t-\gamma}{\alpha}\right)^{\beta-1} \tag{1}$$

Where, β = shape, α = scale, γ = location, t = time, Y = failure rate.

Since WFRF provides a single degradation trend curve and no failure probability distribution, it must be combined with another Bayesian filter, such as PF, to define the failure probability distribution

2.2. Particle filter

PF is a dynamic model that estimates an evolving state of a system over time by incorporating both present and historical data. Unlike static models, sequential models adapt to new data as it becomes available, enabling real-time tracking and prediction. PF integrates observations over time to refine estimates, making it suitable for systems subject to noise, uncertainty, or nonlinearity. PF provides degradation trends, estimation uncertainty, and real-time fault states by leveraging nonlinear and non-Gaussian analysis. PF operates on state-space models, where the model parameters are the observational model and the state-transition model itself, as depicted in Eqs. (2)-(3).

$$f(t|\,\beta,\alpha) = \frac{\beta^j}{\alpha^j}\left(\frac{t}{\alpha^j}\right)^{\beta^j-1} \tag{2}$$

$$\begin{aligned} \beta^j &= f(\beta^{j-1}, v^j) \\ \alpha^j &= f(\alpha^{j-1}, v^j) \end{aligned} \tag{3}$$

Where, β=shape, α=scale, γ=location, v= gaussian noise, t=data point, j= particle.

PF works in five steps: initialization, prediction, weight update, normalization, and resampling. In the initialization step, N particles, along with their weights and initial parameters, are initialized as described in Eqs. (4)-(5). The initial particles are sampled from uniform distributions bounded by the minimum and maximum WFRF parameters obtained from the training datasets. Consequently, the parameters y, β, and α are initialized within the ranges specified for their respective machines. These initialized parameters and weight particles are used to predict trends using Eq. (6) and compare them with the actual degradation curve. During comparison, particles predicted near the degradation curve were given more weight using a likelihood function, as in Eq. (7). Next, the weights are updated based on the likelihood of particles (Eq. (8)) and normalized using Eq. (9). Then, systematic resampling was applied using Eq. (10) to mitigate particle degeneracy and to retain high-probability particles, since particles with negligible weights contribute little to accurate degradation estimation (Labbe, 2020). In this process, the cumulative distribution of normalized particle weights is first computed. A random starting point is then generated within the interval [0, 1/N], followed by the selection of N equally spaced samples from the cumulative weight distribution. Particles with larger weights are replicated more often than particles with negligible weights. This approach maintains particle diversity while improving the stability of state estimation, which is repeated to determine optimized model parameters and estimate trends. Later, a threshold value of degradation provides a probability distribution of failures and estimated EOL. An overview of mechanism of particle filter is shown in Figure 1.

Step 1: Initialization

$$x^j \sim P(x_0) \tag{4}$$

$$w^j = \frac{1}{N} \tag{5}$$

Step 2: Prediction

$$\hat{Y}_k^j = \frac{\beta_k^j}{\alpha_k^j}\left(\frac{t_k}{\alpha_k^j}\right)^{\beta_k^j - 1} \tag{6}$$

$$l = e^{\left(-0.5 * \frac{(Y-\hat{Y})^2}{\sigma^2}\right)} \tag{7}$$

Step 3: Weight update

$$w^j \propto l \tag{8}$$

Step 4: Normalization

$$\widehat{w}^j = \frac{w^j}{\sum_{j=1}^{N} w^j} \tag{9}$$

Step 5: Resampling

$$P\left(w^{*(j)} = x^j\right) = w^j \tag{10}$$

Resampling criterion

$$\left(N_{eff} = \frac{1}{\sum_i w_i^2}\right) < \frac{N}{2} \tag{11}$$

Where, $x =$ parameter, $P(x_0)$ = prior distribution, w = weight, N= particle count, t= time, j= iteration, k= time step.

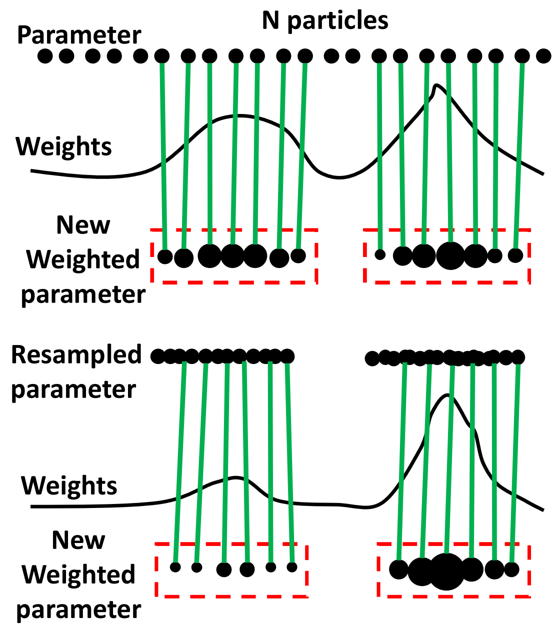

Figure 1. Mechanism of particle filter

2.3. Limitations in existing literature

- Previous studies on machine health monitoring focused on oil analysis that covered inspecting the degradation of oil through various oil testing methods. Similar oil degradation also occurs in the dumper over time. However, vibration analysis has not been examined to estimate oil degradation and predict health in dumpers.
- Similarly, the electric motor is an important element of industry, which suffers from multiple types of faults. Researchers have worked on these faults for diagnostic purposes. However, the prognostic application remains limited due to the need for long-term data collection from unbalanced mass faults and the requirement for accurate prediction.
- Existing studies present WFRF as a statistical model that fits data very well. However, this function provides a single degradation curve and does not specify a probability distribution of degradations, which is required to determine lower and upper bounds of last state before failure. So, the WFRF model requires a probabilistic model that can provide a failure distribution.
- Previous studies on degradation analysis have worked on PF for EOL estimation on various machine elements

been combined with WFRF to estimate degradation and failure probability distribution. Considering the advantages of PF as a Bayesian model and WFRF as a statistical model, a combined approach would be beneficial. Therefore, a hybrid model combining PF and WFRF should be investigated to estimate degradation and EOL.

2.4. Objectives of the study

The aim of this study is to examine degradation analysis and maintenance estimation for various machine types, including dumpers and motors, using vibration signals with a hybrid PF-WFRF model. Therefore, the objectives are completed in four parts:

- To collect vibration data using uniaxial and triaxial accelerometers mounted on two machines, i.e., dumper and motor.
- To establish the most significant frequency band for vibration data for further study using frequency domain analysis, and calculate statistical features from the filtered data.
- To investigate trend analysis in the calculated features from vibration data of two machines and select a significant feature for degradation analysis.
- To model the identified trends using WFRF and PF to determine the posterior distribution based on prior data and initial parameters, and define the probability distribution of maintenance timelines for the dumper and the degradation level in the motor.
- To compare the hybrid PF-WFRF model with the WFRF and XGBoost models to assess EOL estimation.

3. PROPOSED METHODOLOGY

The degradation analysis and EOL estimation using the PF and WFRF models were studied and validated on two different machines: a dumper and an induction motor. The vibration data were collected and processed using signal processing methods, including Fast Fourier Transform (FFT) and RMS calculations. Power Spectral Density (PSD) analysis was performed using the FFT to determine the important frequency band and identify the most significant range for analyzing the trend. The RMS was used to evaluate the trend in the vibration data within the specified frequency band. The RMS trends of the two machines were fed into the PF-WFRF model to train the prior distribution, estimate the posterior distribution of the degradation trend, and determine the respective conditions. The complete framework of the proposed approach is shown in Figure 2.

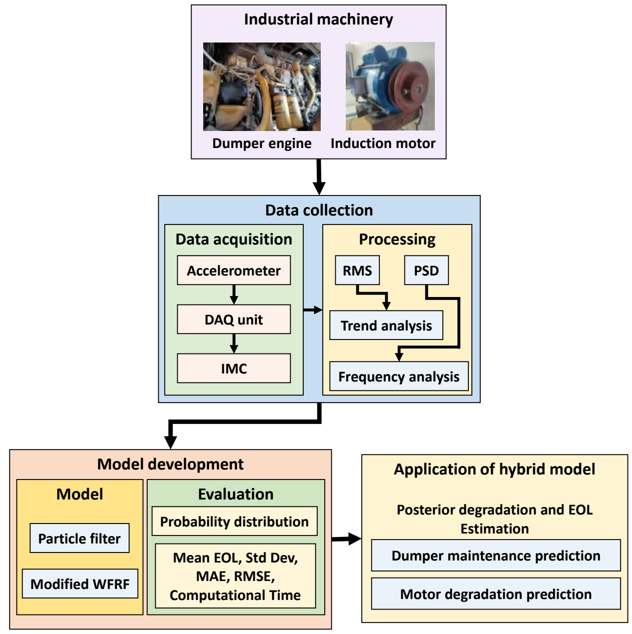

Figure 2. Proposed approach for degradation analysis and EOL estimation

3.1. Data collection

Vibration data was collected from two industrial machines: (1) mining dumper, (2) induction motor. Accelerometers were used to collect vibration data from these machines. These accelerometers were connected to a National Instruments (NI) data acquisition (DAQ) unit (NI 9234 module + NI 9171 chassis), which was later connected to an industrial minicomputer (IMC) and powered through an adapter (Dewangan et al., 2024). This experimental setup was implemented for both machines.

3.1.1. Induction motor vibration data

The experiment was conducted on a single-phase induction motor rated at 1.5 HP, subjected to varying levels of unbalanced load. A triaxial accelerometer was installed at the base of the motor to record vibration at a sampling rate of 10,240 Hz in three directions, i.e., X (transverse direction), Y (axial direction), and Z (vertical direction), as depicted in Figure 3. The unbalanced masses (mass = 2.9 kg) were mounted on the pulley to provide a load to the motor, and the masses were tested at six different levels. For each unbalanced-mass configuration, vibration data were acquired for 15 minutes per day, as depicted in Figure 4. Once the total operating duration reached five hours, the unbalanced mass was increased to the next configuration level, and the procedure was repeated until the final configuration was attained. The masses used in the experiment are listed in Table 4, and unbalance mass configuration is presented in Table 5.

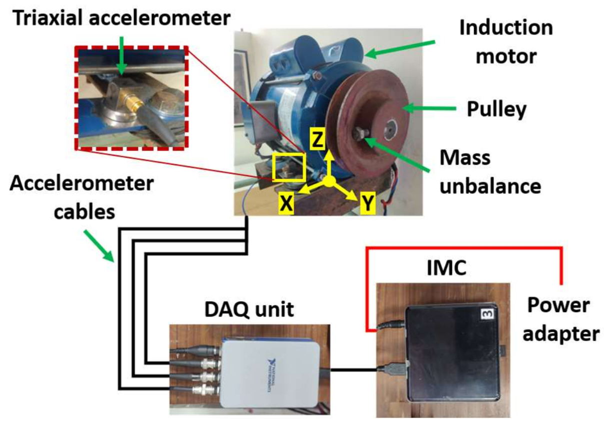

Figure 3. Experimental setup for vibration data acquisition from induction motor

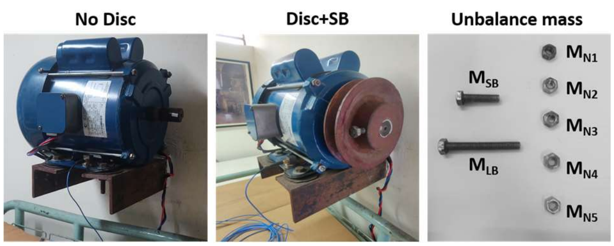

Figure 4. Unbalanced masses used for experiment

Table 4. Unbalance masses

Unbalance	Mass (g)
M_{SB}	25.77
M_{LB}	40.68
M_{N1}	7.91
M_{N2}	8.25
M_{N3}	8.16
M_{N4}	7.61
M_{N5}	6.86

Table 5. Unbalanced mass configuration for experiment

Level	Load condition	Unbalanced mass
L1	No load	No mass
L2	Pulley+ masses	M_{SB}
L3		M_{LB} +M_{N1}
L4		M_{LB} +M_{N1} +M_{N2}
L5		M_{LB} +M_{N1} +M_{N2} +M_{N3}
L6		M_{LB} +M_{N1} + M_{N2} +M_{N3} +M_{N4}
L7		M_{LB} +M_{N1} +M_{N2} +M_{N3} +M_{N4} +M_{N5}

3.1.2. Dumper vibration data

A mining dumper with a capacity of 100 tonnes was selected, and a PCB Piezotronics uniaxial accelerometer (Model: 602D01) was installed on the front right frame to acquire data in the vertical direction, as shown in Figure 5. The sampling rate for the process was fixed at 5,120 Hz. The vibration data was recorded over a long period to cover the dumper's maintenance cycle, which would help study degradation in the dumper. A total of six maintenance cycles, each lasting 20 to 30 days, were captured. During these cycles, the vibration level increased, a phenomenon similar to that reported by Santana et al. (2019). This trend in vibration level was modeled using WFRF. First, the initial parameters of the WFRF model were calculated using five degradation datasets, then used to train the WFRF, allowing the estimation of parameters for an unseen dataset. Later, the PF model was used to determine the degradation trend in the datasets and to estimate the next maintenance schedule based on a defined threshold.

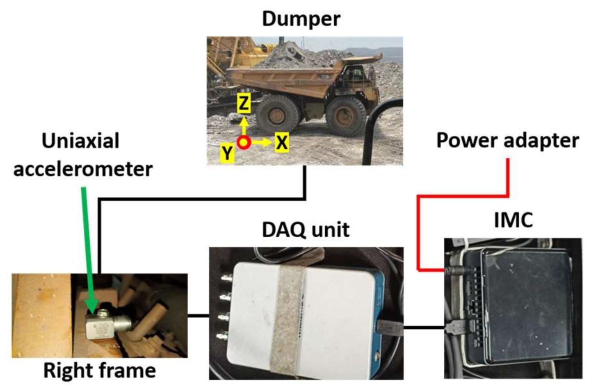

Figure 5. Experimental setup for vibration data acquisition from mining dumper

3.2. Modified WFRF

The modified WFRF equation was derived from Eq. (1) by putting γ = 0 and introducing an additional constant term, y, to account for vibration data that do not originate at zero. The inclusion of y enables the model to represent the non-zero baseline vibration level commonly observed under normal operating conditions. In actual vibration monitoring, degradation indicators often exhibit an initial offset due to machine dynamics and measurement conditions. Therefore, the parameter y represents the initial degradation level, while shape parameter (β) governs the degradation behavior and scale parameter (α) controls the characteristic degradation timescale. The values of β, α, and y would characterize the degradation behavior. Consequently, the modified WFRF retains the degradation characteristics of the original Weibull function while providing improved flexibility in modeling vibration degradation trends. The modified WFRF was used to model degradation of machine components. Eq. (12) represents the modified WFRF.

$$Y = y + \frac{\beta}{\alpha^{\beta}} t^{\beta-1} \tag{12}$$

Where, y=initial constant, β=shape, α=scale, Y = output

Further, the modified WFRF was formulated using a state-space model to define degradation and the probability distribution of failures, with the observation model (Eq. (13)) defining the degradation and the state transition model (Eq. (14)) specifying the parameters of the modified WFRF. The process noise v_y, v_β, and v_α were assumed to follow zero-mean Gaussian distributions $N(0,\sigma^2)$ with standard deviations of 0.2, 0.2, and 0.2 corresponding to the selected motion model parameters. Additionally, the value of standard deviation (σ) for likelihood is 0.05 in Eq. (7).

$$Y_j = y_j + \frac{\beta_j}{\alpha_j^{\beta_j}} t^{\beta_j - 1} \tag{13}$$

$$\begin{aligned} y_j &= y_{j-1} + v_{y,j} \\ \beta_j &= \beta_{j-1} + v_{\beta,j} \\ \alpha_j &= \alpha_{j-1} + v_{\alpha,j} \end{aligned} \tag{14}$$

Where, y=constant, β=shape, α=scale, v= process noise, t=data point, j= particle.

3.3. Process of EOL estimation

The degradation in the dumper during the maintenance cycle was assessed using the RMS vibration level from activity tracking. These degradation trends were used to estimate EOL for the next maintenance, using a hybrid approach that integrates a PF with WFRF. The complete approach is shown in Figure 6 and detailed in section 2.2. The process began with initialization, in which a set of particles representing the parameters of a WFRF degradation model derived from RMS trends during the maintenance cycle was generated, with N particles having equal weights. During the estimation phase, the current model parameters were used to predict the system's behavior. In the prediction step, new WFRF parameters were forecast using prior estimates. The update phase adjusted particle weights based on the new predictions. If the convergence criterion, i.e., number of iterations, was not met, the resampling step regenerated particles based on their weights to avoid particle degeneracy.

Once convergence was achieved, the updated parameters were passed to the EOL estimation part. This part used the measured RMS levels of the recognized activity to estimate WFRF model parameters using PF. Subsequently, the estimated parameters were incorporated into the WFRF model to project degradation trends for N particles up to a predefined failure threshold; i.e., the estimated trend fails when it reaches the threshold. This enabled the estimation of EOL for each particle trajectory and the derivation of an EOL Probability Density Function (PDF) using Eq. (15), thereby providing both the most probable failure time and the associated prediction uncertainty. This methodology was used for validation and EOL estimation on vibration data.

For the motor vibration data, the hybrid model was examined on 100 particles and 100 iterations. Further, hyperparameters were varied, with iterations ranging between 50, 100, and 150, and particle counts ranging between 50, 100, and 150. Similarly, for the dumper vibration data, the hybrid model was examined on 100 particles and 500 iterations. Further, hyperparameters were varied, with iterations ranging between 50, 100, and 150, and particle counts ranging between 100, 300, and 500. Later, estimated EOLs were compared with actual EOLs using various metrics, including mean, standard deviation (STD), Mean Absolute Error (MAE), and Root Mean Squared Error (RMSE), as defined in Eqs. (16)-(19).

Furthermore, a comparative analysis was conducted between standalone WFRF and XGBoost-WFRF to assess the effect of using PF-WFRF for EOL estimation using the above-discussed metrics.

$$\hat{p}(\text{EOL}) = \frac{1}{Nh}\sum_{j=1}^{N} K\left(\frac{EOL - EOL_j}{h}\right) \tag{15}$$

$$Mean = \frac{\sum_j p_j EOL_j}{\sum_j p_j} \tag{16}$$

$$Std = \sqrt{\frac{\sum_j p_j \left(EOL_j - \mu_{EOL}\right)^2}{\sum_j p_j}} \tag{17}$$

$$MAE = \frac{1}{N}\sum_{j=1}^{N}\left|EOL_j - EOL_{actual}\right| \tag{18}$$

$$RMSE = \sqrt{\frac{1}{N}\sum_{j=1}^{N}\left(EOL_j - EOL_{actual}\right)^2} \tag{19}$$

Where, $\hat{p}$ = PDF, K= kernel density function, N = particle count, h = bandwidth, j =particle, p = probability

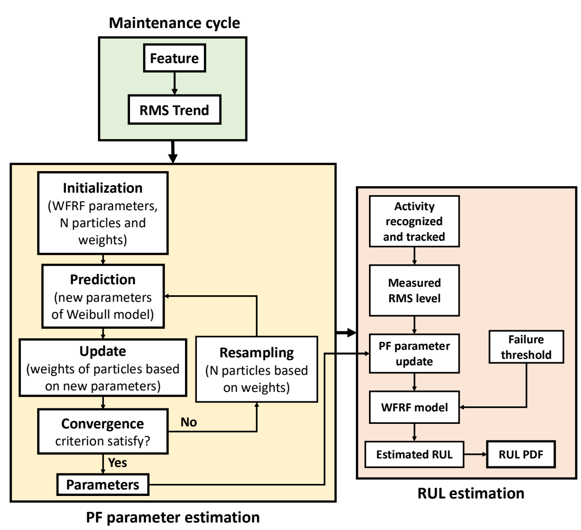

Figure 6. PF-WFRF approach for EOL estimation

4. RESULTS AND DISCUSSION

The operation of the proposed PF-WFRF hybrid model is demonstrated using vibration data from two different machine configurations: a mining dumper and an electric motor. First, vibration data from a motor were collected and analyzed to identify a significant frequency range affected by unbalanced masses. Second, the vibration data from a dumper was analyzed to correlate with maintenance data.

4.1. Induction motor degradation

4.1.1. Vibration signal analysis

The collected vibration data for X, Y, and Z directions are shown in Figure 7, where legends L1-L7 represent the unbalanced mass configuration used in the experiment. PSD was used to identify significant frequency components in the spectrum, revealing that amplitudes are most significant in the 1-800 Hz range across all measurements and unbalanced masses. So, this range was selected to further analyze degradation and predict EOL from vibration data.

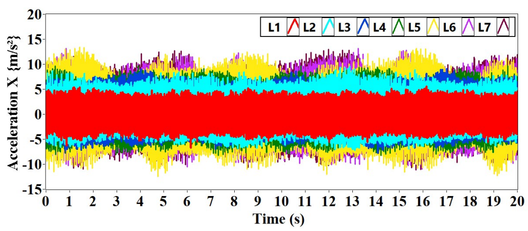

(a)

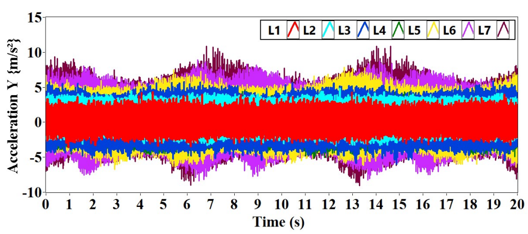

(b)

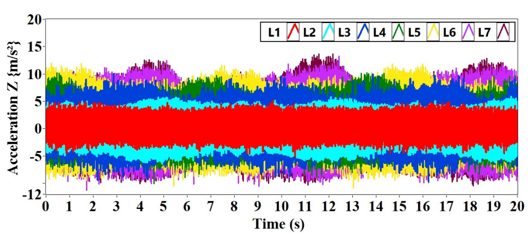

(c)

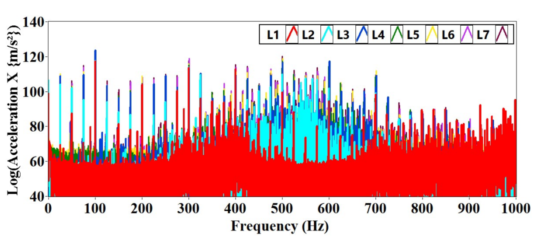

(d)

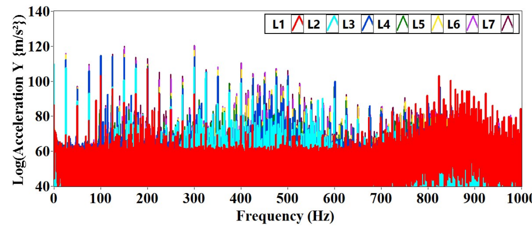

(e)

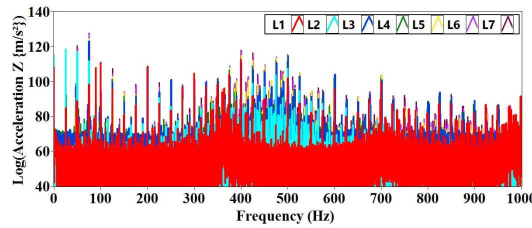

(f)

Figure 7. (a-c) Acceleration signal and (d-f) PSD for various unbalanced masses from Table 5

4.1.2. Feature extraction

RMS values were extracted from all collected vibration data, which showed an increasing trend over time and unbalanced masses due to degradation and unbalanced forces, as depicted in Figure 8. In L1 condition, with neither load nor mass, the vibration level was below 2.5 m/s^2. For other conditions, the vibration level increased and reached 6.5 m/s^2 due to degradation and unbalance. Therefore, overall motor degradation was monitored under this condition, and EOL was estimated. For that, the vibration trend was segmented into six parts and modeled using the proposed method to execute the task, as shown in Figure 9.

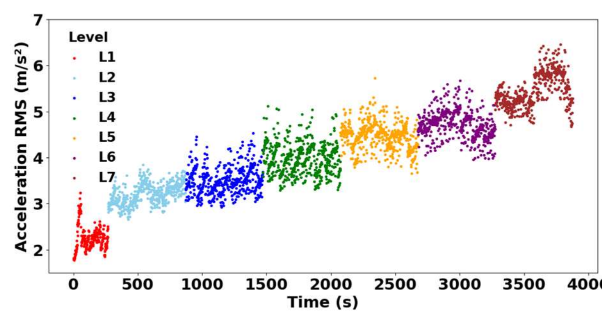

Figure 8. Resultant RMS of electric motor under various unbalanced masses

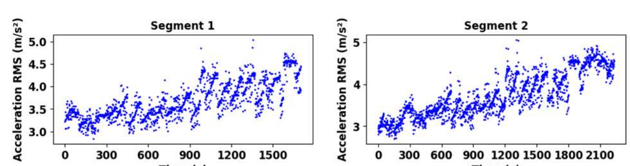

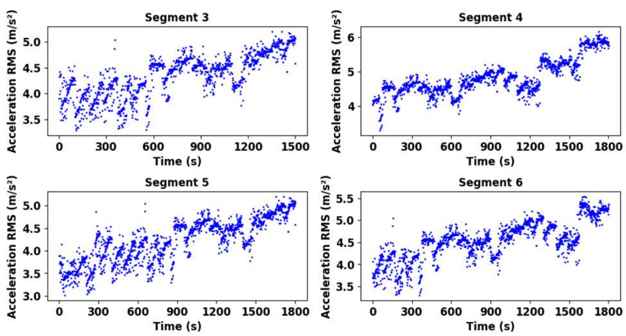

Figure 9. RMS trends of electric motor acceleration signal for various unbalanced masses

4.1.3. Unbalance-condition estimation

RMS levels from all unbalanced masses were modeled using PF-WFRF, and six segments were used as input to PF. Initial WFRF parameters extracted from the remaining segments were fed to PF, which requires initialization. Additionally, a uniformly distributed weight was assigned to each particle and updated at each iteration. The parameters of WFRF models obtained by the least squares method are provided in Table 6, the initial parameters are illustrated in Table 7, and the RMS trend used to showcase the maintenance estimation is shown in Figure 10(a). Initially, 100 particles were used to start PF estimation, with WFRF parameters uniformly sampled from maximum and minimum values for each parameter. WFRF parameters were iteratively optimized using 100 iterations. The trends estimated from PF are shown in Figure 10(b). The failure threshold for the induction motor was selected as the RMS vibration level observed at the end of the final unbalanced-mass configuration (L7), which represented the most severe operating condition examined in the experiment. Since this configuration exhibited the highest vibration level and corresponded to the maximum degradation state achieved during testing, the associated RMS value of 5.9 m/s² was adopted as the failure criterion for EOL estimation. Using a defined threshold, mean maintenance time (based on estimated trends) and the actual maintenance time (based on the threshold) were very close, with a difference of nearly 117 seconds, indicating predictive performance in Figure 10(c). Moreover, a PDF of estimated EOL is presented to define the distribution of estimates. The estimated parameters and their histogram are shown in Figure 10(d), and the parameter values for these estimates are provided in Table 8. The density plot and table show that the particle population was concentrated around the true values of Y, while α and β exhibited wider distributions due to uncertainty in the degradation timescale. This was due to the distribution of estimated EOLs, which ranged from 3000 to 5000 seconds; the farthest estimated EOL received the lowest weightage, whereas those near the actual EOL received higher weightage. Moreover, estimated EOLs earlier than the actual EOL received higher weightage, as shown in Figure 10(d), indicating that early maintenance could be performed on the machine.

Table 6. Parameters estimated for motor RMS trends

Segment	Y	β	α
1	3.282	2.590	135.547
2	3.098	2.330	97.164
3	3.862	2.169	71.475
4	4.503	4.500	492.105
5	3.466	1.858	36.741
6	3.468	2.326	6.214

Table 7. Initial parameters of WFRF

Range	Y	β	α
Min	3.098	1.326	6.214
Max	4.503	4.500	492.105

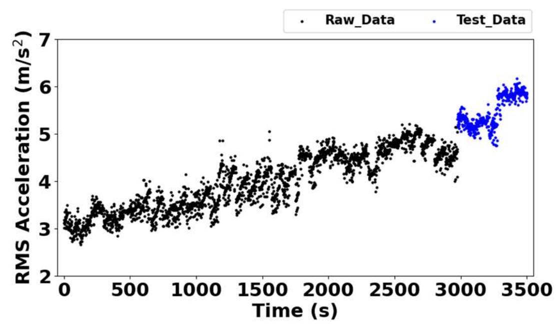

(a)

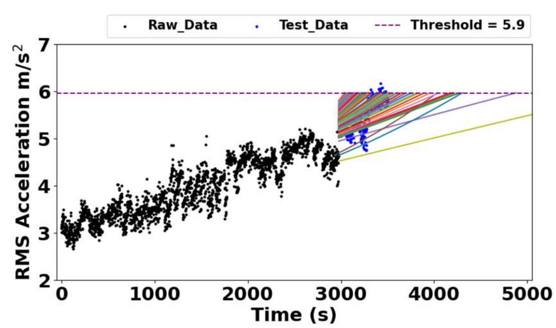

(b)

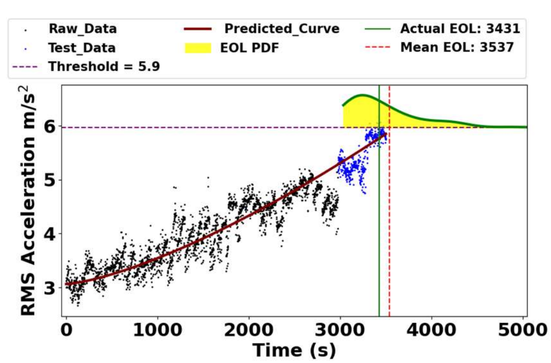

(c)

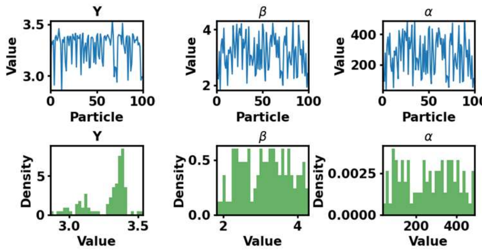

(d)

Figure 10. Estimated EOL from RMS vibration trend of motor: (a) RMS vibration level, (b) estimated trends and threshold level, (c) estimated EOL time with PDF of estimated trends, and (d) WFRF parameter density

Table 8. Estimated WFRF parameter for RMS trend

Parameter	True value	Min	Max
Y	2.948	2.86	3.50
β	1.873	1.82	4.34
α	40.905	33.23	434.21

Further, a sensitivity analysis was conducted to assess the effects of the PF hyperparameters (particle count and number of iterations) on EOL estimation, as shown in Table 9. For that, 50, 100, and 150 iterations were considered; similarly, 50, 100, and 150 particle counts were considered. As the number of iterations increased from 50 to 150, the predicted mean EOL converged towards the actual EOL, while the standard deviation, MAE, and RMSE decreased, respectively. This indicates that additional iterations allow the particle weights to converge more effectively towards the observed degradation trend, thereby improving prediction accuracy and reducing uncertainty. Similarly, increasing the particle count from 50 to 150 improved EOL distribution, reducing MAE and RMSE. Although a higher particle count increases the computational cost, it provides more accurate and stable EOL estimates. Therefore, 100 iterations and 100 particles yielded the best prediction performance for the investigated motor vibration data.

Table 9. Parametric evaluation of PF on EOL estimation

PF Hyperparameter		**Metrics**			
		Mean EOL	Std deviation	MAE	RMSE
Motor (Actual EOL = 3431)					
Iteration	Particle count				
50	100	3592	447.41	323.66	478.47
100	100	3482	447.75	317.17	465.69
150	100	3476	402.15	306.19	435.95
Particle count	Iteration				
50	100	3605	432.33	374.97	490.32
100	100	3482	447.75	317.17	465.69
150	100	3453	391.48	278.66	396.37

4.2. Dumper maintenance estimation

4.2.1. Vibration signal analysis

Vibration data from the right frame of the dumper were much noisier than those from the electric motor. Data correlated with maintenance data, in which lubricating oil, filters, and engine seals are replaced at every scheduled maintenance. A portion of the collected vibration data from the dumper is shown in Figure 11.

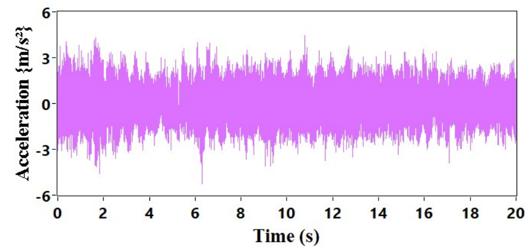

(a)

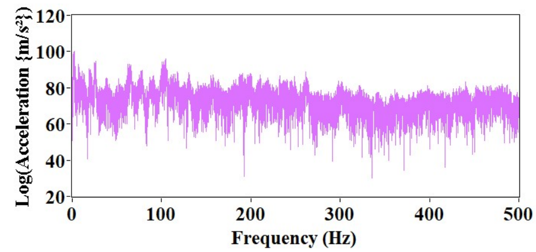

(b)

Figure 11. Right frame (a) acceleration signal and (b) PSD

4.2.2. Feature extraction

Vibration data were analyzed using an RMS statistical feature calculated over the 100 Hz frequency range, which was then correlated with maintenance data. During dumper operation, lubricant and other components degrade, increasing vibration until next maintenance. This increment in vibration level was monitored over time to determine the next maintenance time and its probability distribution. Vibration levels for six such maintenance cycles are presented in Figure 12, where vibration across all segments increased due to lubricant degradation and other supporting elements. This increase in vibration level was predicted using the proposed method.

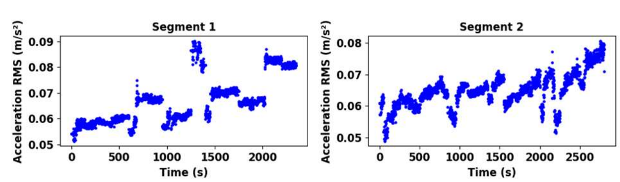

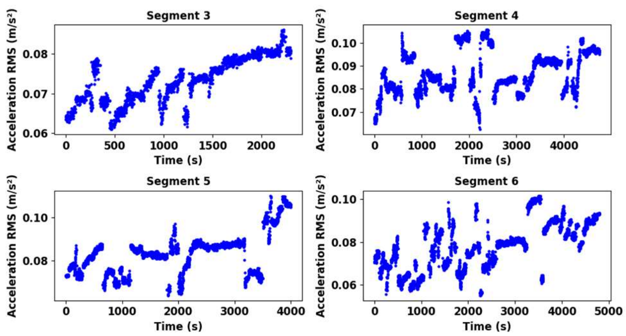

Figure 12. RMS trends from right frame vibration signal for maintenance cycles

4.2.3. Maintenance estimation

One of the segments of right frame, 'Segment 3', was modeled using PF-WFRF, and the other five were used as input for PF. Initial WFRF parameters extracted from the remaining segments were fed to PF, which requires initialization. Additionally, a uniformly distributed weight was assigned to each particle and updated at each iteration. The parameters of WFRF models obtained by the least squares method are provided in Table 10, the initial parameters are illustrated in Table 11, and the RMS trend used to showcase the maintenance estimation is shown in Figure 13(a). Since one degradation trend from each vibration dataset, from the right frames, was selected for demonstration, the remaining datasets were used to extract WFRF parameters to initialize PF. Initially, 100 particles were used to start PF estimation, with WFRF parameters uniformly sampled from maximum and minimum values for each parameter. WFRF parameters were iteratively optimized using 500 iterations. The trends estimated from PF are shown in Figure 13(b). The failure threshold for the dumper was selected as the RMS vibration level measured immediately before scheduled maintenance. At this stage, the lubricating oil and associated components had reached the end of their service interval, resulting in the highest vibration level within the maintenance cycle. Therefore, the RMS value of 0.083 m/s² was adopted as the threshold for EOL estimation. Using a defined threshold, mean maintenance time (based on estimated trends) and the actual maintenance time (based on threshold) were very close, with a difference of nearly 98 seconds, indicating predictive performance in Figure 13(c). Moreover, a PDF of estimated EOL is presented to define the distribution of estimates. The estimated parameters and their histogram are shown in Figure 13(d), and the parameter values for these estimates are provided in Table 12. The density plot and table show that the particle population was concentrated around the true values of Y, while α and β exhibited a wider distribution due to uncertainty in the degradation timescale. This was due to the distribution of estimated EOLs, which ranged from 1800 to 2900 seconds; the farthest estimated EOL received the lowest weightage, whereas those near the actual EOL received higher weightage. Moreover, estimated EOLs earlier than the actual EOL received higher weightage, as shown in Figure 13(d), indicating that early maintenance could be performed on the machine.

Table 10. Parameters estimated for right-frame RMS trends

Segment	Y	β	α
1	0.056	2.129	513.590
2	0.062	7.303	2185.929
3	0.067	2.848	933.801
4	0.047	1.083	37.972
5	0.080	11.659	3248.215
6	0.066	2.204	984.804

Table 11. Initial parameters of WFRF

Range	Y	β	α
Min	0.047	1.083	37.972
Max	0.080	7.303	3248.215

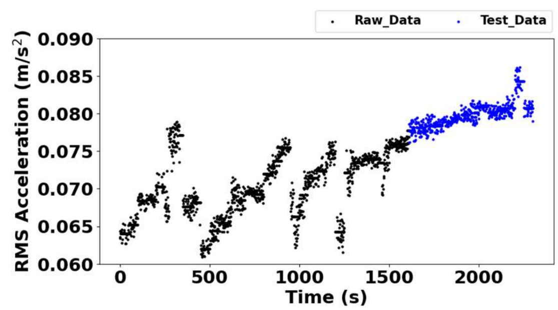

(a)

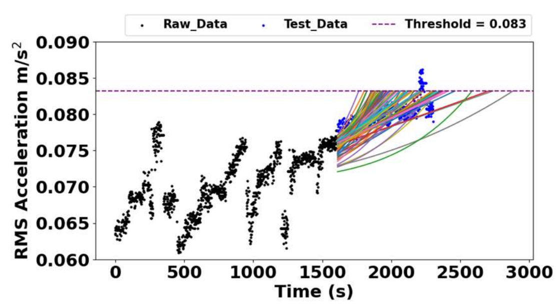

(b)

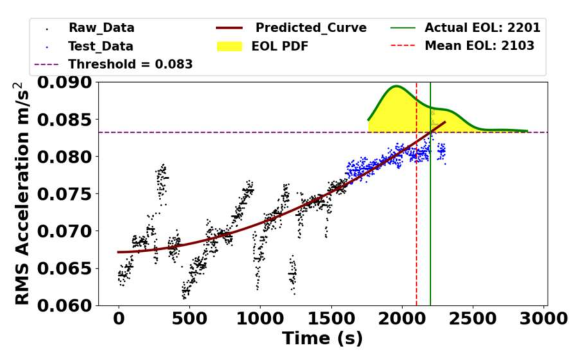

(c)

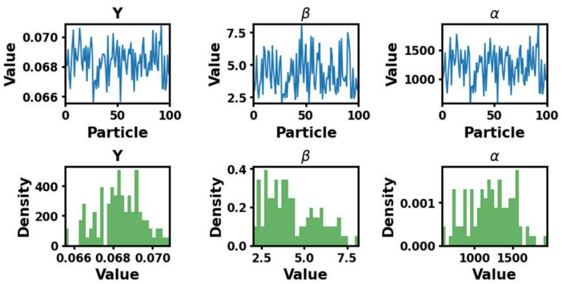

(d)

Figure 13. Estimated EOL from RMS vibration trend of right frame: (a) RMS vibration level, (b) estimated trends and threshold level, (c) estimated maintenance time with PDF of estimated trends, and (d) WFRF parameter density

Table 12. Estimated WFRF parameter for RMS trend

Parameter	True value	Min	Max
Y	0.066	0.065	.070
β	2.204	2.041	8.152
α	984.804	580.60	1948.17

Further, a sensitivity analysis was conducted to assess the effects of the PF hyperparameters (particle count and number of iterations) on EOL estimation, as shown in Table 13. For that, 100, 300, and 500 iterations were considered, whereas 50, 100, and 150 particle counts were considered. Increasing the number of iterations from 100 to 500 progressively improved prediction accuracy by reducing standard deviation, MAE, and RMSE, indicating better convergence. Similarly, increasing the particle count improved the representation of the posterior parameter distribution and reduced prediction errors, even at a higher computational cost. Overall, 100 particles and 500 iterations provided a balance among prediction accuracy, uncertainty, and computational time for dumper vibration data.

5. DISCUSSION

The results demonstrated that the proposed PF-WFRF framework effectively estimates degradation progression and EOL under both controlled and industrial operating conditions. PF recursively updated WFRF parameters based on available degradation information, thereby converging the weighted particles toward the actual degradation trend. Consequently, particles representing unrealistic degradation received lower weights over iterations, whereas particles corresponding to the observed degradation received higher weights. This adaptive updating mechanism enabled the framework to progressively reduce uncertainty and improve EOL estimation as the machine approaches failure.

The estimated WFRF parameters for motor and dumper provided a physical interpretation of the degradation behavior, as illustrated in Table 8 and Table 12. Since WFRF shape parameter (β) greater than unity indicates increasing degradation, the estimated β values for both the induction motor (β = 1.82-4.34) and the dumper (β = 2.041-8.152) confirmed that vibration levels increased as the machine approached their respective failure thresholds. The larger β values obtained for the dumper indicated a faster increase in vibration severity than for the induction motor, highlighting a more rapid deterioration process during actual field operating conditions. In contrast, the lower β values for the motor resulted in a gradual increase of degradation under controlled unbalance conditions.

Table 13. Parametric evaluation of PF on EOL estimation

PF Hyperparameter		Metrics			
		Mean EOL	Std deviation	MAE	RMSE
Dumper (Actual EOL = 2201)					
Iteration	Particle count				
100	100	2621	1133.39	480.59	1202.73
300	100	2472	800.41	452.85	822.21
500	100	2103	217.65	206.38	239.74
Particle count	Iteration				
50	500	2411	389.13	386.44	330.67
100	500	2103	217.65	206.38	239.74
150	500	2288	198.43	192.19	207.28

The scale parameter (α) governs the degradation timescale and influences the rate at which the degradation evolves, as illustrated in Table 8 and Table 12. The induction motor exhibited relatively smaller α values (α = 33.23-434.21), indicating that the degradation trend evolved over a shorter timescale. Conversely, the dumper showed larger α values (α = 580.60-1948.17), suggesting that the degradation evolved over a longer operating period before reaching the failure threshold. The wider range of α values observed for the dumper also reflects the variability associated with changing conditions in field applications. Therefore, the estimated β and α parameters not only provide an accurate statistical representation of the vibration trends but also correspond to the physical degradation characteristics of the investigated systems.

Furthermore, the uncertainty distributions generated by PF provide information not available from deterministic approaches, as illustrated in Figure 10 and Figure 13. The concentrated distribution of higher-weight particles near the actual EOL demonstrates that PF effectively identifies the most probable degradation trends while simultaneously quantifying prediction uncertainty as a PDF of EOL estimations. Furthermore, several high-probability EOL estimates occurred before the actual failure time, where such predictions enable maintenance activities to be scheduled before failure occurs.

The comparative evaluation with standalone WFRF and XGBoost-WFRF further highlights the advantages of the proposed approach, as shown in Table 14. The deterministic WFRF model provided a physically interpretable representation of degradation but could not handle uncertainty in EOL estimation. Conversely, XGBoost-WFRF offers data-driven prediction capability but lacks accuracy in predicting WFRF parameters due to limited data. By integrating the degradation modeling capability of WFRF with the probabilistic estimation capability of PF, the proposed PF-WFRF framework provided both improved prediction accuracy and uncertainty quantification, and worked effectively with limited data, whereas ML models require large amounts of data. Although the deterministic WFRF model produced lower prediction errors for the selected degradation segments, it provides only a single EOL estimate and cannot quantify uncertainty. In contrast, PF-WFRF generates probabilistic EOL distributions and confidence bounds, which are advantageous for maintenance decision-making under uncertain operating conditions. The lower prediction errors across both machine datasets demonstrate that the hybrid framework maintains robust performance under both controlled laboratory and industrial operating conditions. Additionally, the computational requirements of these models have been studied, with PF-WFRF being more efficient than XGBoost-WFRF for both motor and dumper EOL prediction.

Further, PDF of the estimated EOLs generated by the PF-WFRF framework provided insights for maintenance scheduling. Instead of relying on a single deterministic failure time, maintenance decisions can be based on the distribution of predicted EOL values. Higher-weight EOL estimates that occur before the actual failure time yield conservative maintenance recommendations, allowing maintenance activities to be scheduled before failure. In addition, narrower EOL distributions for the dumper provided more confidence in maintenance decisions, whereas wider distributions for the motor indicated uncertainty in the degradation process and would require increased monitoring.

Therefore, the results highlight that the proposed PF-WFRF framework is capable of accurately predicting EOL across both controlled (motor) and noisy industrial (dumper) environments. The consistent performance across these two distinct datasets demonstrates the robustness and generalizability of the approach. Furthermore, the probabilistic nature of the model provides not only point estimates but also uncertainty bounds, which are essential for reliable decision-making in PHM applications.

6. CONCLUSION AND FUTURE SCOPE

This study examined degradation of machine components, such as dumper engine components due to aging and electric motor due to unbalanced masses. The degradation was modeled using a hybrid PF-WFRF model, and EOL was estimated for the dumper and the electric motor. PF helped estimate uncertainty in EOL using PDFs and parameters based on the initial WFRF parameter, while WFRF provided a non-linear degradation model. The estimated PDFs were right-skewed for both the dumper and the motor, i.e., components would reach their EOL earlier than their actual lifetimes. Moreover, PDF helped define the period during which EOL would occur. Further, the estimated WFRF parameters were close to the actual WFRF parameters from degradation curve through PF. The results demonstrated the applicability of the proposed approach to both smoother and noisy datasets for predicting EOL.

This paper has some limitations. The present study considered only vibration sensors as indicators of degradation. However, other parameters also change due to machine degradation, such as oil and current levels, which should be considered together for optimized prediction, given their combined effects: vibration, oil, and current. Further, the initial failure model parameters of WFRF were required to determine the degradation curves; these parameters can be removed using techniques such as a genetic algorithm-based grid search. Moreover, PF is computationally intensive, particularly in high-dimensional state spaces, because it requires maintaining a large particle population to ensure accurate estimation.

Table 14. Comparison of PF-WFRF with WFRF and XGBoost-WFRF for EOL estimation

Model	**Metrics**				**Computational time (s)**
	Mean EOL	Std deviation	MAE	RMSE	
	Motor (Actual EOL = 3431)				
WFRF	3501	--	--	--	167
PF-WFRF	3482	447.75	317.17	465.69	4068
XGBoost-WFRF	3618	509.05	487.08	517.18	11686
	Dumper (Actual EOL = 2201)				
WFRF	2301	--	--	--	191
PF-WFRF	2103	217.65	206.38	239.74	7730
XGBoost-WFRF	2537	594.31	377.16	583.59	28004

REFERENCES

Ahmad, W., Ali Khan, S., & Kim, J. M. (2017). A hybrid prognostics technique for rolling element bearings using adaptive predictive models. *IEEE Transactions on Industrial Electronics*, *65*(2), 1577–1584. doi: 10.1109/TIE.2017.2733487

Cameron, Z. A., & Krantz, T. L. (2023). Statistical distribution of gear surface fatigue lives at high reliability. *International Journal of Fatigue*, *167*(PB), 107350. doi: 10.1016/j.ijfatigue.2022.107350

Chen, T., & Guestrin, C. (2016). XGBoost: A scalable tree boosting system. *Proceedings of the ACM SIGKDD International Conference on Knowledge Discovery and Data Mining*, *August 201*, 785–794. https://doi.org/10.1145/2939672.2939785

Cheng, Z. (2015). A hybrid prognostics approach to estimate the residual useful life of a planetary gearbox with a local defect. *Journal of Vibroengineering*, *17*(2), 682–694. doi: 10.21595/jve.2014.15240.

Cuesta, J., Leturiondo, U., Vidal, Y., & Pozo, F. (2025). A review of prognostics and health management techniques in wind energy. *Reliability Engineering and System Safety*, 260. doi: 10.1016/j.ress.2025.111004

de Souza, L. G. P., de Castro Cesário, M., Ribeiro, R. R. C., Ferreira, J. R., & de Paiva, A. P. (2025). A simulation-based method for cutting tool reliability estimation without experimental replications. *International Journal of Advanced Manufacturing Technology*, 1749–1764. doi: 10.1007/s00170-025-17181-4

Dewangan, N., Agrawal, A. K., Siddiqui, M. A. H., & Chattopadhyaya, S. (2019). Degradation analysis of gear oil SAE 90 used in load haul dumper machine. *IOP Conference Series: Materials Science and Engineering*, *624*(1). doi: 10.1088/1757-899X/624/1/012011

Dewangan, N., Mohanty, A. R., & Kumar, R. (2024). Dump truck activity recognition using vibration signal and convolutional neural network. *Automation in Construction*, *165*. doi: 10.1016/j.autcon.2024.105495

Dey, S., Mandal, S. K., & Bhar, C. (2017). Analysis of factors, which influence the cycle time of dumpers of open cast coal mines to improve production. *Advances in Modelling and Analysis A*, *78*(3), 289–302. doi: 10.18280/mmc_c.780303

Fricke, K., Nascimento, R. G., Corbetta, M., Kulkarni, C. S., & Viana, F. A. C. (2023). Prognosis of Li-ion batteries under large load variations using hybrid physics-informed neural networks. *Proceedings of the Annual Conference of the Prognostics and Health Management Society, PHM*, *15*(1), 1–12. doi: 10.36001/phmconf.2023.v15i1.3463

Guo, J., Li, Z., & Li, M. (2020). A review on prognostics methods for engineering systems. *IEEE Transactions on Reliability*, *69*(3), 1110–1129. doi: 10.1109/TR.2019.2957965

Gupta, N., Tandon, N., Pandey, R. K., Vidyasagar, K. E. C., & Kalyanasundaram, D. (2020). Tribological and vibration studies of textured spur gear pairs under fully flooded and starved lubrication conditions. *Tribology Transactions*, *63*(6), 1103–1120. doi: 10.1080/10402004.2020.1794093

Hachem, H., Vu, H. C., & Fouladirad, M. (2024). Different methods for RUL prediction considering sensor degradation. *Reliability Engineering and System Safety*, *243*(June), 109897. doi: 10.1016/j.ress.2023.109897

Jafari, S., & Byun, Y. C. (2022). XGBoost-based remaining useful life estimation model with extended kalman particle filter for lithium-ion batteries. *Sensors*, *22*(23), pp. 1–18. doi: 10.3390/s22239522

Jin, Z., Li, X., Qiu, Z., Li, F., Kong, E., & Li, B. (2025). A data-driven framework for lithium-ion battery RUL using LSTM and XGBoost with feature selection via Binary Firefly Algorithm. *Energy*, *314*(November 2023). doi: 10.1016/j.energy.2024.134229

Kang, Z., Catal, C., & Tekinerdogan, B. (2021). Remaining useful life (RUL) prediction of equipment in production lines using artificial neural networks. *Sensors (Switzerland)*, *21*(3), 1–20. doi: 10.3390/s21030932

Khan, S., Yairi, T., Tsutsumi, S., & Nakasuka, S. (2024). A review of physics-based learning for system health management. In *Annual Reviews in Control* (Vol. 57). doi: 10.1016/j.arcontrol.2024.100932

Khine, M. H. H., Kim, C. G., & Aunsri, N. (2025). A review of Bayesian-filtering-based techniques in RUL prediction for Lithium-Ion batteries. *Journal of Energy Storage*, *111*, 115371. doi: 10.1016/j.est.2025.115371

Kundu, P., Darpe, A. K., & Kulkarni, M. S. (2019). Weibull accelerated failure time regression model for remaining useful life prediction of bearing working under multiple operating conditions. *Mechanical Systems and Signal Processing*, *134*. doi: 10.1016/j.ymssp.2019.106302

Labbe, R. (2014). *Kalman and bayesian filters in python*. Chap, *7*(246), 4.

Li, S., Fang, H., & Shi, B. (2021). Remaining useful life estimation of lithium-ion battery based on interacting multiple model particle filter and support vector regression. *Reliability Engineering and System Safety*, *210*(January), 107542. doi: 10.1016/j.ress.2021.107542

Li, X., Ding, Q., & Sun, J. Q. (2018). Remaining useful life estimation in prognostics using deep convolution neural networks. *Reliability Engineering and System Safety*, *172*(October), 1–11. doi: 10.1016/j.ress.2017.11.021

Mohanty, A. R., Pradhan, P. K., Mahalik, N. P., & Dastidar, S. G. (2012). Fault detection in a centrifugal pump using vibration and motor current signature analysis. *International Journal of Automation and Control*, *6*(3–4), 261–276. doi: 10.1504/IJAAC.2012.051884

Nectoux, P., Gouriveau, R., Medjaher, K., Ramasso, E., Chebel-Morello, B., Zerhouni, N., & Varnier, C. (2012). PRONOSTIA: An experimental platform for bearings accelerated degradation tests. *IEEE*

International Conference on Prognostics and Health Management, PHM'12, *May 2014*, 1–8. http://hal-obspm.ccsd.cnrs.fr/UNIV-BM/hal-00719503

Pal, R. S. C., Dewangan, N., & Mohanty, A. R. (2023). Fault diagnosis of induction motors: an architecture for real-time assessment as a cyber-physical system. *Engineering Transactions*, *71*(1), 1–20. doi: 10.24423/EngTrans.2243.20230112

Pradhan, P. K. (2014). *Condition monitoring of submersible pump using motor current signature analysis*. Doctoral dissertation. Indian Institute of Technology Kharagpur, Kharagpur, India.

Qiu, H., Lee, J., Lin, J., & Yu, G. (2006). Wavelet filter-based weak signature detection method and its application on rolling element bearing prognostics. *Journal of Sound and Vibration*, *289*(4–5), 1066–1090. doi: 10.1016/j.jsv.2005.03.007

Rai, V. K., & Mohanty, A. R. (2007). Bearing fault diagnosis using FFT of intrinsic mode functions in Hilbert-Huang transform. *Mechanical Systems and Signal Processing*, *21*(6), 2607–2615. doi: 10.1016/j.ymssp.2006.12.004

Rathore, M. S., & Harsha, S. P. (2022). Prognostic analysis of high-speed cylindrical roller bearing using Weibull distribution and k-nearest neighbor. *Journal of Nondestructive Evaluation, Diagnostics and Prognostics of Engineering Systems*, *5*(February), 1–12. doi: 10.1115/1.4051314

Rezamand, M., Kordestani, M., Carriveau, R., Ting, D. S. K., & Saif, M. (2020). An integrated feature-based failure prognosis method for wind turbine bearings. *IEEE/ASME Transactions on Mechatronics*, *25*(3), 1468–1478. doi: 10.1109/TMECH.2020.2978136

Salinas-Camus, M., Goebel, K., & Eleftheroglou, N. (2025). A comprehensive review and evaluation framework for data-driven prognostics: Uncertainty, robustness, interpretability, and feasibility. *Mechanical Systems and Signal Processing*, *237*(June), 113015. doi: 10.1016/j.ymssp.2025.113015

Santana, C. M. (2022). Correlation between vibration level, lubricating oil viscosity and total number base of an internal combustion engine operated with gasoline and ethanol. *SAE Technical Papers*, 1–8. doi: 10.4271/2022-01-0620

Santana, C. M., Mautone, J., & Almeida, H. (2019). Analysis of the increase level of vibration in an internal combustion engine due to the degradation of the lubricating oil. *SAE Technical Papers*, *2019-April*(April). doi: 10.4271/2019-01-0780

Siddiqui, M. A. H., Pal, S. K., Dewangan, N., Chattopadhyaya, S., Sharma, S., Nekoonam, S., & Issakhov, A. (2021). Sludge formation analysis in hydraulic oil of load haul dumper 811MK V machine running at elevated temperatures for bioenergy applications. *International Journal of Chemical Engineering*, *2021*, 1–14. doi: 10.1155/2021/4331809

Skordilis, E., & Moghaddass, R. (2020). A double hybrid state-space model for real-time sensor-driven monitoring of deteriorating systems. *IEEE Transactions on Automation Science and Engineering*, *17*(1), 72–87. doi: 10.1109/TASE.2019.2921285

Wang, Y., He, L., Jiang, S., & Chow, T. W. S. (2021). Failure prediction of hard disk drives based on adaptive rao-blackwellized particle filter error tracking method. *IEEE Transactions on Industrial Informatics*, *17*(2), 913–921. doi: 10.1109/TII.2020.3016121

Wang, Y., Peng, Y., & Chow, T. W. S. (2021). Adaptive particle filter-based approach for RUL prediction under uncertain varying stresses with application to HDD. *IEEE Transactions on Industrial Informatics*, *17*(9), 6272–6281. doi: 10.1109/TII.2021.3051285

Zhu, R., Peng, W., Wang, D., & Huang, C. G. (2022). Bayesian transfer learning with active querying for intelligent cross-machine fault prognosis under limited data. *Mechanical Systems and Signal Processing*, *183*(February). doi: 10.1016/j.ymssp.2022.109628

BIOGRAPHIES

Nagesh Dewangan is a Ph.D. Student in the Department of Mechanical Engineering at the Indian Institute of Technology (IIT) Kharagpur, India. He received the B.E. degree in Mechanical Engineering from the Bhilai Institute of Technology, India, in 2016, and the M.Tech. degree in Maintenance Engineering & Tribology from the Indian Institute of Technology (Indian School of Mines) Dhanbad, India, in 2019. His research interests include machinery condition monitoring, fault diagnosis and prognosis, signal processing, machine learning, cyber-physical systems, and edge computing.

Amiya Ranjan Mohanty is a Professor in the Department of Mechanical Engineering at the Indian Institute of Technology (IIT) Kharagpur, India. He received the B.Sc. Engineering (Hons.) degree in Mechanical Engineering from the National Institute of Technology Rourkela, India, in 1986, M.Tech. degree in Machine Design from the Indian Institute of Technology Kharagpur, India, in 1988, and Ph.D. in noise control from the University of Kentucky, Lexington, USA, in 1993. He has worked as a Postdoctoral Fellow in active noise control at the Ray W. Herrick Laboratories, School of Mechanical Engineering, Purdue University, West Lafayette, USA. He has also worked in the R&D division of Larsen and Toubro Limited in Mumbai and at Ford Motor Company in Detroit, USA. His research interests include machinery condition monitoring, acoustics and noise control, underwater acoustics, machine design, and automobile engineering. He is currently serving as the BIS Standardization Chair Professor at the IIT Kharagpur.